OPEN

EXPERIMENTAL

Establishing a Reproducible Hypertrophic Scar following Thermal Injury: A Porcine Model

Scott J. Rapp, MD
Aaron Rumberg, BS
Marty Visscher, PhD
David A. Billmire, MD
Ann S. Schwentker, MD
Brian S. Pan, MD

Background: Our complete understanding of hypertrophic scarring is still deficient, as portrayed by the poor clinical outcomes when treating them. To address the need for alternative treatment strategies, we assess the swine animal burn model as an initial approach for immature scar evaluation and therapeutic application.
Methods: Thermal contact burns were created on the dorsum of 3 domestic swine with the use of a branding iron at 170°F for 20 seconds. Deep partial-thickness burns were cared for with absorptive dressings over 10 weeks and wounds evaluated with laser and negative pressure transduction, histology, photographic analysis, and RNA isolation.
Results: Overall average stiffness (mm Hg/mm) increased and elasticity (mm) decreased in the scars from the initial burn injury to 8 weeks when compared with normal skin ($P < 0.01$). Scars were thicker, more erythematous, and uniform in the caudal dorsum. The percent change of erythema in wounds increased from weeks 6 to 10. Histology demonstrated loss of dermal papillae, increased myofibroblast presence, vertically oriented vessels, epidermal and dermal hypercellularity, and parallel-layered collagen deposition. Immature scars remained elevated at 10 weeks, and minimal RNA was able to be isolated from the tissue.
Conclusions: Deep partial-thickness thermal injury to the back of domestic swine produces an immature hypertrophic scar by 10 weeks following burn with thickness appearing to coincide with the location along the dorsal axis. With minimal pig to pig variation, we describe our technique to provide a testable immature scar model. *(Plast Reconstr Surg Glob Open 2015;3:e309; doi: 10.1097/GOX.0000000000000277; Published online 19 February 2015.)*

Hypertrophic scarring is an unpredictable and poorly understood sequela in both the pediatric and adult populations. Defined as raised, thick, hyperemic, and indurated tissue that does not extend beyond the boundaries of the scar, hypertrophic scarring is frequently seen in secondarily healed burn wounds and after skin-incising surgical procedures. The initial presentation often clinically arises around 8 weeks.[1] The etiology is not completely defined; however, it is thought that there is an exaggerated proliferation phase with abnormal collagen deposition, leading to nodular structures composed of contracting myofibroblasts and small vessels.[2]

Clinically, treatment and the prevention of hypertrophic scars are wrought with unsatisfactory results. Noninvasive treatment often yields to noncompliance through the burdensome application of pressure garments, silicone therapy, and massage.[3–6] Invasive interventions such as surgical excision/tissue rearrangement, laser therapy, or radiation are

From the Division of Plastic and Reconstructive Surgery, Shriner's Hospital for Children, Cincinnati Children's Hospital Medical Center, Cincinnati, Ohio.
Received for publication November 4, 2014; accepted January 5, 2015.

DOI: 10.1097/GOX.0000000000000277

Disclosure: *The authors have no financial interest to declare in relation to the content of this article. The Article Processing Charge was paid for by the authors.*

not applicable to larger surface area scarring. Moreover, these modalities can lead to recurrence or further reduction in acceptable cosmesis.

With successful clinical applications lacking, returning to an animal model may be beneficial for further evolution in scar understanding. Creating a reproducible, consistent, and easily testable animal model so that new treatment modalities can quickly be implemented in our burn population has become a focus at our institution. The domestic swine represents such an animal model that is cost effective and has similar skin characteristics to humans. We report on the feasibility of creating hypertrophic scarring to serve as a platform for examining future treatment options.

METHODS

Institutional Animal Care and Use Committee approval was obtained at our institution under the protocol number: 1d12106. Three 8-week-old domestic swine were purchased from Schwab Farms (Wilmington, Ohio) and individually housed in the Animal Research Core at Cincinnati Children's Hospital Medical Center. The initial weights of the pigs were around 90 lb and around 200 lb at the time of killing. Cincinnati Children's Hospital Medical Center maintains a current Animal Welfare Assurance with the US Department of Health and Human Services, Office of Laboratory Animal Welfare. A Medium Duty "BF-125-S" 125 Watt Electric Handheld Branding Tool with a 3″ × 1″ head was purchased from Brand-First (Madison Heights, Mich.) (Fig. 1).

All animals had their backs shaved clean of any hair and were prepared sterilely after general anesthesia induction (Fig. 2A). One dose of preoperative antibiotics was given to each animal, with no prophylactic dosing following injury. The branding iron was paired with a thermocoupler (Brand-First), and the temperature was set to 170°F after being measured with a digital thermometer by conduction.

Approximately 5 cm from the midline and over the latissimus dorsi and paraspinal muscles, a 3″ × 1″ rectangular deep partial-thickness burn was created by thermal injury after applying the branding tool for 20 seconds. The branding tool was positioned such that gravity alone was the downward force when creating each burn. The branding iron's temperature was recalibrated after each burn to ensure similar initial contact heat. Each animal received 20 total test areas (10 per side). Wounds were dressed with bacitracin, adaptic, and absorptive gauze. To address the difficulty of keeping the wounds clean and prevent further contact injury and abrasion while being housed, the animals were wrapped circumferentially in Coban elastic dressing (3M, St. Paul, Minn.). All eschars were allowed to autodebride, and no intervention was performed on chronic granulation tissue. Buprenorphine was administered during surgery, and fentanyl patches were placed under a tegaderm to provide improved drug delivery.

Scars were evaluated with weekly digital photography using fixed distance and light conditions, acquired with a Nikon D-90 camera, a Micro-Nikkor 60-mm lens, and a Nikon R1 wireless close-up flash system (Nikon, Melville, N.Y.). A 3D camera was also

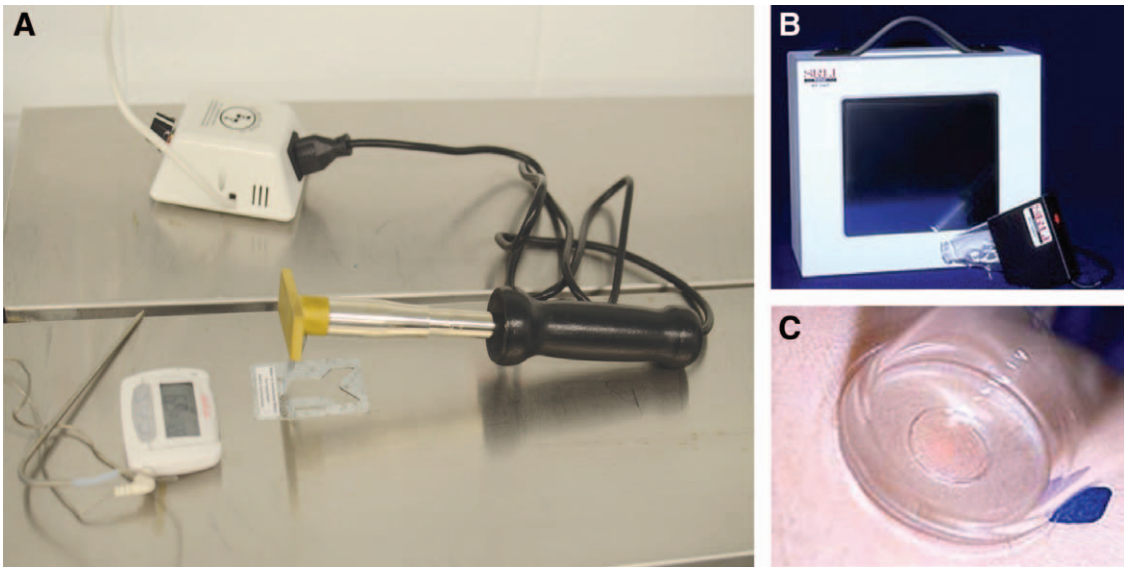

Fig. 1. Thermal injury was created by a branding iron. Temperature was regulated to 170°F and dermal contact for 20 seconds. A, Downward force was through gravity alone. B and C, Skin tissue pliability and compliance were measured with a negative pressure transducer.

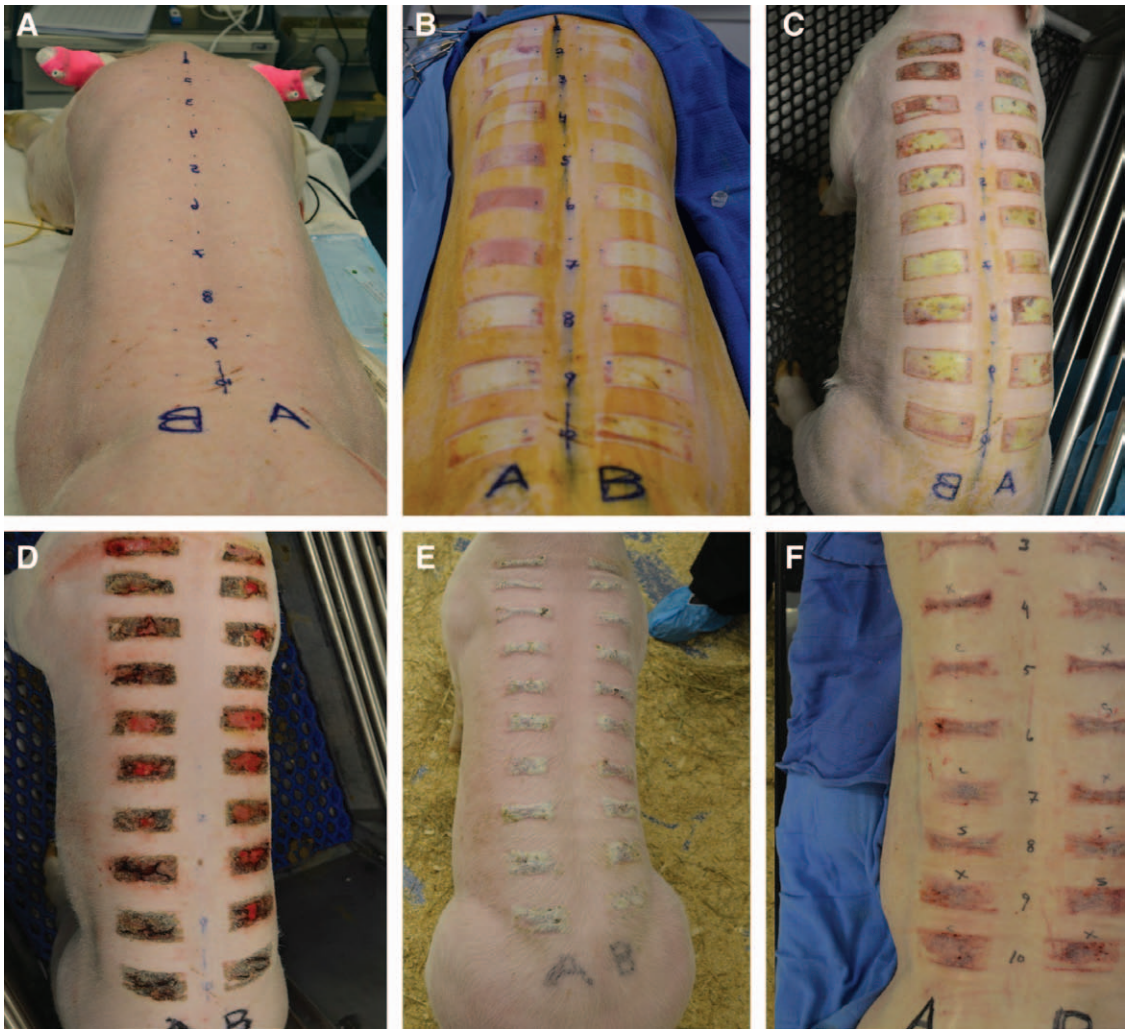

Fig. 2. Photographic evaluation of contact burns: preoperative (A), day 0 (B), 1 week post burn (C), 3 weeks post burn (D), 5 weeks post burn (E), and 8 weeks post burn (F). Eschar was present until around 6 weeks before raised hyperemic tissue was observed (F).

implemented to determine the ability to capture large surface area variations for future analysis. Erythema to the scar tissue was determined, measured with Image J Software (National Institute of Health), setting the threshold to include only red pixels. Scar stiffness and elasticity were determined and measured with the BTC-2000 device (SRLI Technologies, Nashville, Tenn.). This device works by using a laser beam to precisely calculate the height of a tissue deformation dome created by applying a suction vacuum on the skin.[7] Stiffness, measured in mm Hg/mm, is the mechanical behavior of the structure and calculated from the slope of the linear region in the pressure-deformation curve. Elasticity is the recovery or reverse deformation (mm) that occurs immediately upon the full release of negative pressure.

Four-millimeter full-thickness punch biopsies were performed on all scars at weeks 1, 2, 6, and 10. Half of the samples were placed in RNAlater (Life Technologies, Grand Island, N.Y.) and the other half in formalin for tissue processing. Samples were embedded in paraffin and stained with hematoxylin and eosin to evaluate cellularity and vascularity and Masson's trichrome for collagen content. Immunohistochemistry for alpha smooth muscle actin (α-SMA) was performed on samples to evaluate myofibroblast presence. Samples frozen in RNAlater at −80°C had the RNA isolated and evaluated with the use of an RNeasy Mini-kit (Qiagen, Valencia, Calif.).

RESULTS

Qualitative Wound Characteristics

Immediately following burn injury, dermal elements were observed in the wound with no adipose tissue penetrating the deep reticular dermis (Fig. 2B). By 2 weeks, a thick eschar was present on all wounds with granulation tissue and no new hair

growth by week 5 (Fig. 2E). The adherent portions of the eschar were allowed to autodebride with no intervention. There were no clinical infections and no antibiotics used outside the perioperative period. By week 10, all eschars were replaced with intact epidermis and a scar not extending beyond the confines of the original burn (Fig. 2F).

Scar morphology differed based on its location on the dorsum. A 3D camera was used to test the ability to detect minor differences in scar topography along the dorsal axis (Fig. 3A). In all 3 pigs, the thermal injury that was created over the scapula near the head resulted in a less prominent, less erythematous scar and appeared to have greater scar contraction (Fig. 3B). The central portions of the scar were more narrowed when compared with inferior scars. Conversely, scars on the caudal portion of the dorsum were elevated the greatest, with no evidence of contraction from the original insult (Fig. 3C). Further, obtaining a biopsy through the most central portion of scar and into the subcutaneous fat with the standard 4-mm punch biopsy proved difficult as a result of the thickened tissue.

Standardized photographs of each scar were compared over time and erythema captured with Image J analysis. Overall redness to the wounds increased each week up to 4 weeks. During weeks 4–6, the erythema slightly improved. However, from week 6 to week 10, the overall mean redness to each wound continued to increase (Fig. 4). Hyperemia was also noted to be more pronounced in the caudal injuries at 10 weeks when compared with the cranial injuries when comparing the amount of red pixilation percentage in each wound (Fig. 3). The cranial third scars ($n = 6$) to animal 1 had an average red pixilation of 94.03% the surface area of the scar. This is significantly lower than the caudal third ($n = 6$) demonstrating 92.16% ($P < 0.05$). Animal 2 had cranial scars ($n = 6$) with 96.13% red pixels to 94.35% in the caudal scars ($n = 6$). Animal 3 had cranial scars with 94.51% red pixels to 90.62% in the caudal area. The average percent difference between top third and bottom third scars for all animals was 2.5% at 10 weeks ($n = 18$ scars).

Wound Histology

On hematoxylin and eosin staining, unburned skin demonstrates definable epidermal layers, papillary and reticular dermis with rete pegs, and adnexal structures (Fig. 5A). The collagen stained with Masson's trichrome demonstrates a whirled pattern or "basket weave" appearance (Fig. 5B). Burned animal skin at 2 weeks shows disruption to the previously definable layers, with evidence of necrotic elements in the dermis (Fig. 5C). There is an influx of neutrophils and flattening of papillary dermis (Fig. 5D). By week 10, the epidermal and dermal layers are both hypercellular and thickened versus normal unburned skin with return of deep-penetrating rete pegs (Fig. 5E). There is no return of adnexal structures, and collagen deposition is more robust with layering parallel to the skin surface (Fig. 5F).

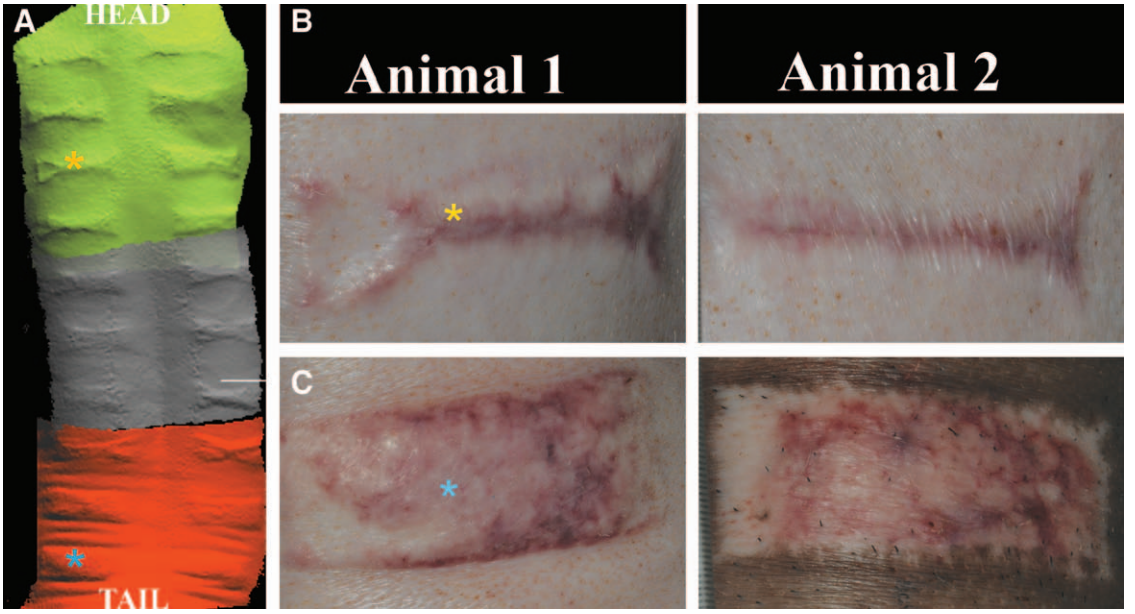

Fig. 3. 3D scans of dorsum demonstrate elevated scar at 8 weeks (A). Morphology to the hypertrophic scar varied based on dorsal position. Caudally positioned burns resulted in more uniform/raised scar (C) vs narrow, irregular-shaped scar tissue cranially (B).

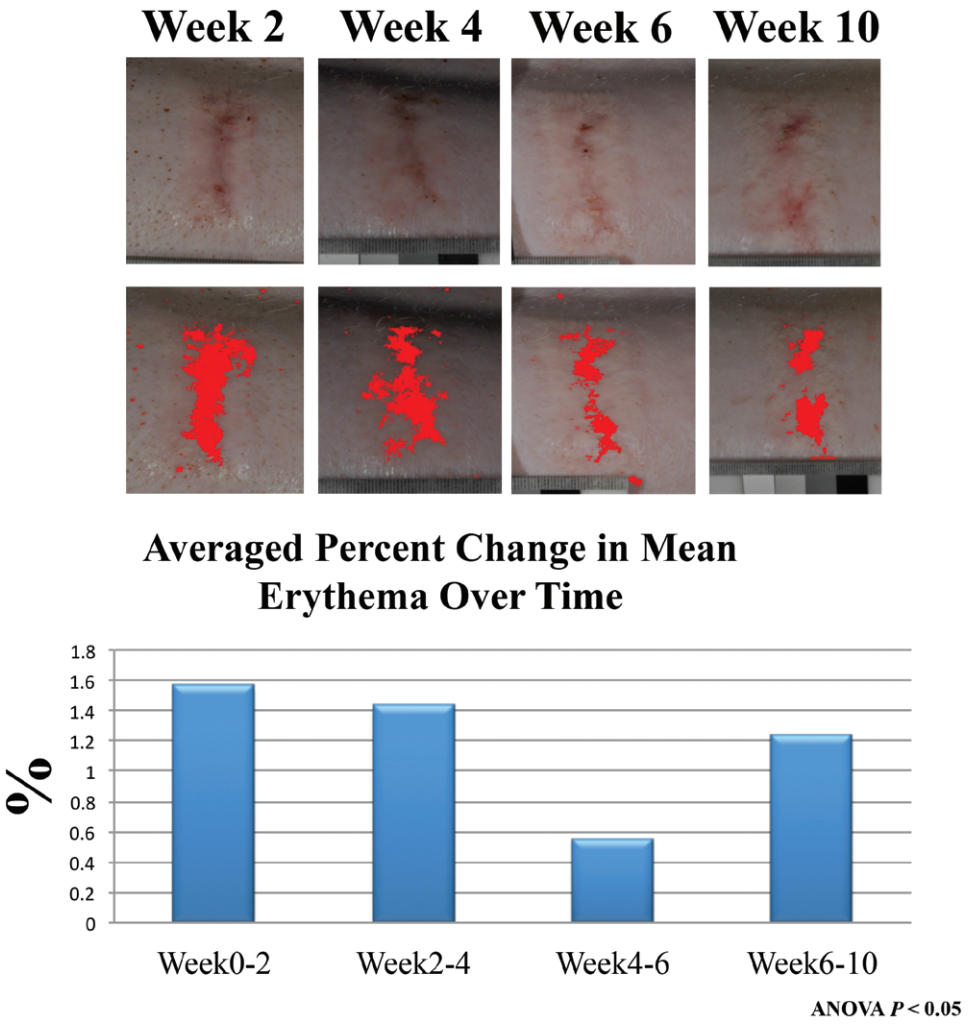

Fig. 4. Image J software was used to quantify the amount of erythema to each scar with means averaged and percent change over time calculated. Redness to the scars decreased from weeks 4–6 overall, but continued to increase in erythema following up to 10 weeks.

Immunohistochemistry labeling for α-SMA expression was performed to observe myofibroblast presence. In unburned skin, myofibroblasts are circumscribing vessels in the papillary dermis (Fig. 6A). Deep in the reticular dermis, there seems to be a paucity of a subdermal plexus. After 2 weeks, burned skin shows an influx of inflammatory cells and vascular penetration deep in the reticular dermis (Fig. 6B). Surrounding the vessels again is the presence of α-SMA uptake, suggesting a greater presence of myofibroblasts. By week 10, inflammatory cells have diminished, and the vessels have taken a vertically oriented pattern perpendicular to the skin surface (Fig. 6C). Again, myofibroblasts seem to be present deep into the reticular dermis with a less established papillary dermis vascular complex seen in unburned skin (Fig. 6, arrow).

Biomechanics

Negative transduction pressure measurements were captured with the BTC-2000, revealing differences in stiffness and elasticity to the wounds. The overall elasticity revealed a 29%, 38%, and 34% reduction in elastic deformation (mm) when compared to the adjacent unburned skin at 2, 4, and 10 weeks, respectively ($P < 0.01$) (Fig. 7). Stiffness measurements were increased at each time point in burned skin relative to normal unburned untreated skin. The mechanical behavior of the scar tissue demonstrates an 8.6% increase in mm Hg/mm at 2 weeks. The proportional degree of stiffness did not change when evaluated up to 10 weeks post injury (Fig. 8).

RNA Isolation

RNA was quantified in each scar to determine the amount of cellular activity present. At 2 weeks,

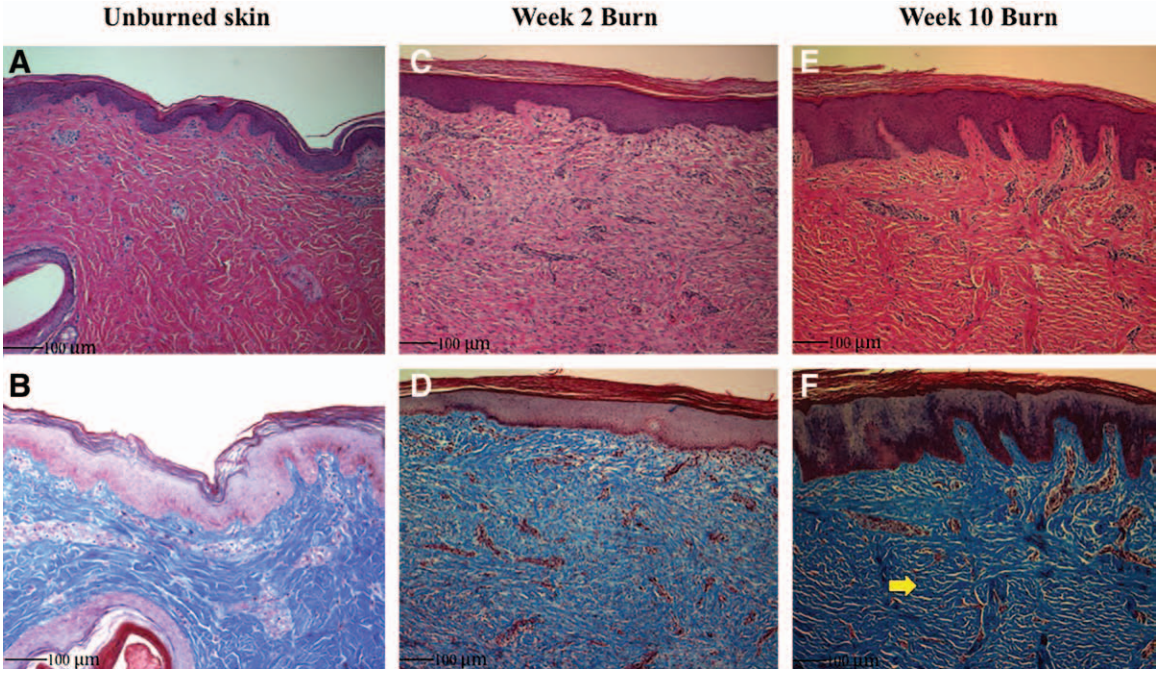

Fig. 5. Hematoxylin and eosin and trichrome staining. A, Swine dorsal skin demonstrates a dermal thickness similar to human skin. B, The collagen layering is in basket weave appearance. C and D, After 2 weeks, burned skin shows a neutrophil infiltrate, vascular ingrowth, and loss of rete pegs. E, Hypercellularity, thickened epidermis/dermis, and vertically oriented vessels deep into the reticular dermis are present after 10 weeks of healing. F, The collagen fibers become parallel in their layered orientation to the skin edge (arrow).

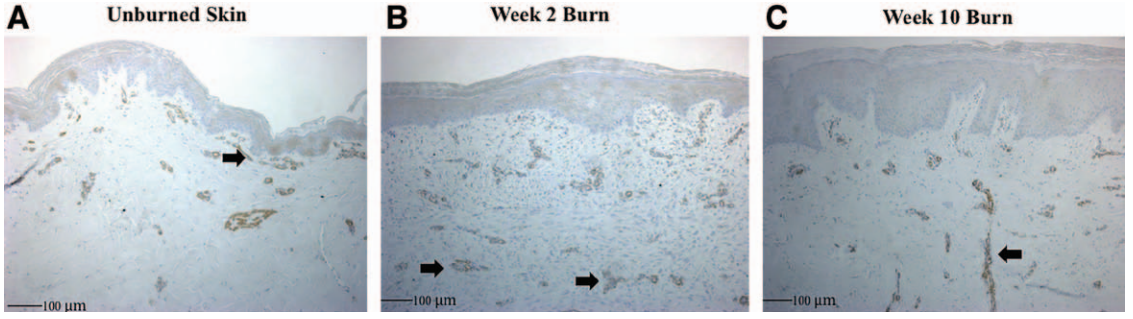

Fig. 6. A, Unburned animal skin shows myofibroblasts as brown staining in the subdermal complex after labeling with α-SMA antibody. B, There is greater penetration of vessels by week 2 post burn and increased α-SMA uptake deep into the reticular dermis (arrow). C, By week 10, the vessels have become vertically oriented, perpendicular to the skin surface with apparent increased myofibroblast presence.

ample RNA with good quality could be extracted. Pig 1 and Pig 2 had 233 and 369 ng/µl, respectively, with a ratio of absorbance of 2. The quantity was enough for microarray and RNA sequencing. Tissue process from all following sample dates provided an inadequate amount of RNA for further processing.

DISCUSSION

To provide for quick translational application, an ideal animal model for comparative medicine is one that closely resembles the histologic features, immunology, cellular signaling and composition, clinical behavior, and biochemistry to that of human tissue.[8] Primates, rats, dogs, and rabbits have all been described as models, each with their espoused advantages and limitations.[9–11] Cost and ethical concern make dogs and primates unfavorable for a widespread model. Although rabbit, rat, and mice models benefit from the ease of care and cost, the wound healing physiology has not been demonstrated to be the most similar to humans. The above small animals have less developed dermal vascularity, thinner epithelium, and flattened dermal-epidermal junctions, with wounds primarily healing by contraction.[12] Implanting human scar tissue onto nude mice holds interesting promise, but reproducibility has yet to be established.[13]

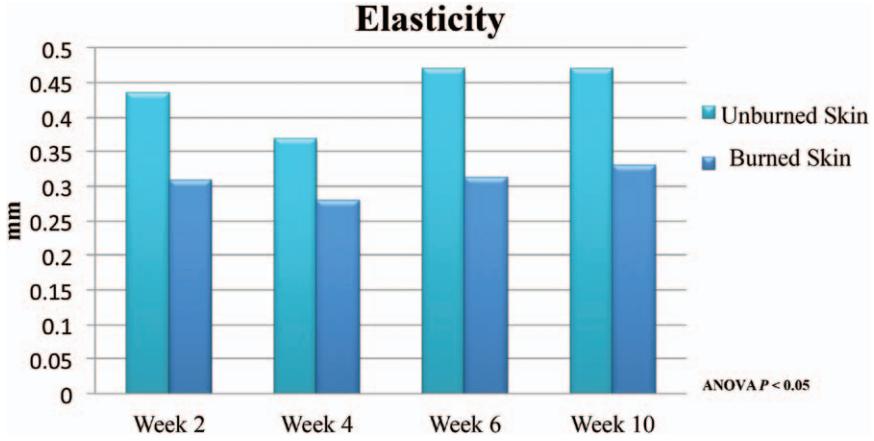

Fig. 7. Elasticity, or reverse deformation, was measured with the BTC-2000, demonstrating no significant improvement in scar up to 6 weeks post injury.

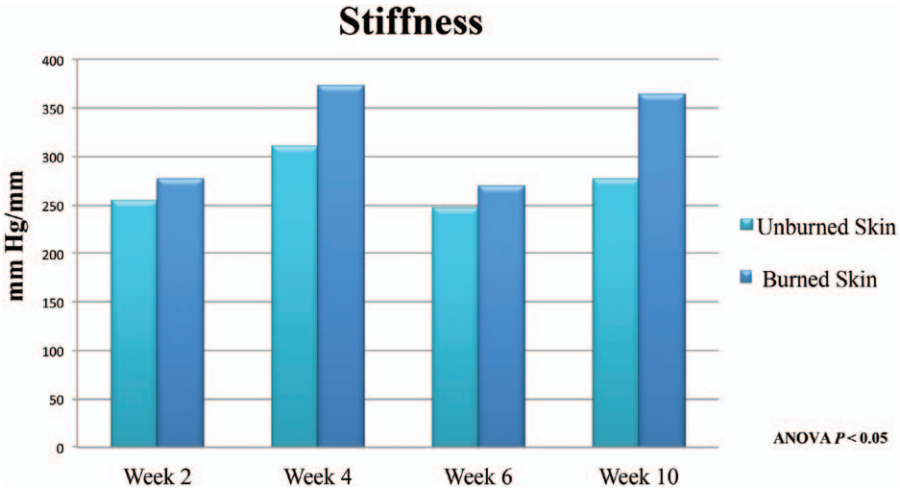

Fig. 8. Stiffness or material property of the tissue demonstrates decreased pliability up to 10 weeks post burn when averaged and compared to normal skin in animal subjects.

Porcine wound healing and its comparison to human tissue healing has been reported frequently in the literature, highlighting similarities in histology and immunohistochemistry.[14–16] Such comparable features allow for the swine model to be used as a precursor to human trials. Pigs are large enough to provide ample tissue for culture and analysis and have similar skin characteristics to humans in regard to epidermal/dermal thickness and nerve composition.[9,17] Wound healing times are also parallel, such as the time to reepithelialization.[18] Further, in multiple reported porcine wound models, hypertrophic scarring characteristics including thickness and hyperemia are clinically most similar to humans.[14] Immunologically, xenografts and acellular swine biologic skin substitutes are commonly used in burn victims and for abdominal wall reconstruction.

Our goal in this pilot study was to develop a model that could be used to further investigate alternative interventions on hypertrophic scars. Serving a large population of pediatric burn patients at our institution, it has not been our experience that all outside institutional burns are being treated in a routine fashion or according to accepted standards. We often see results from largely untreated burns leading to hypertrophic scaring and those resulting from inadequate initial debridement and grafting. As such, we are looking to optimize treatment options in addition to conventional techniques. We have anecdotally seen an observed improvement in scar healing maturation and quality following autologous fat injections in the clinical setting. Adipose-derived fat cells have shown capabilities to assist in regenerative medicine.[19–21] Laser therapy may also serve a role to improve overall characteristics to scars.[22] Both of the above are now part of our ongoing studies with this wound model.

The 3D scanner was able to capture an accurate and detailed image portraying the elevation of each

scar. Images from multiple time points could be overlaid, and theoretically, the volume change to each scar could be quantified. This was attempted in this model; however, the rapid growth of the pigs made superimposing the images difficult and thus results were not included. The Vancouver Scar Scale is widely recognized as a standard method to qualitatively evaluate burn scars.[23] However, this evaluation technique relies on individual observers and personal interpretation to judge and rate the amount of erythema in a wound. To offset observer bias for scar evaluation, we used Image J software to add a quantitative component as an adjunct to visual clinical evaluation. An objective measurement can be deduced from the type of pixels that are present in a photograph using standardized light and distance parameters. Overall redness of the wounds increased each week up to 4 weeks. During weeks 4–6, the erythema slightly improved. The reasoning behind this remains unclear although it may be due to low sampling size. However, anecdotally, the senior authors have observed this phenomenon in immature burn scars clinically where scars will seem to improve before getting worse.

Mechanical stress testing revealed a decrease in elasticity to the wound and increase in stiffness. Elasticity measures the amount of elastic recovery or reverse deformation (mm) that occurs immediately upon the full release of negative pressure. Stiffness or modulus determines the mechanical behavior of the tissue independent of its shape or size. Stiffness was determined from the slope of the linear region in the pressure-deformation curve. Although only measured within 10 weeks following injury, the lack of improvement to both elasticity and stiffness suggests prolonged healing phase without amelioration seen in a normal wound-healing curve. It is possible that the short observation time did not allow for enough remodeling of the wound to show improvement in these biomechanical parameters. Capturing time points further out from the point of injury would help standardize the inflammation and remodeling phase curve in this animal model. Moreover, it would be useful to correlate age with mechanical testing in future studies to account for dermal/epidermal changes over time. We plan to extend the sampling time period past 12 months in ongoing studies.

The goals of histologic analysis were to determine if immature scars up to 10 weeks began developing characteristics similar to those established in the literature that exist for hypertrophic scarring in humans. Before thermal injury, the swine epidermal/dermal junction, vascular composition, and dermal thickness are similar to humans. Thermally injured tissue at 10 weeks demonstrated a change in cellular composition and collagen layering similar to other reports.[24] The collagen layers are thicker and oriented parallel to the skin surface. There is hypercellularity and epidermal/dermal thickening with a loss of adnexal structures. Vessels are present in higher density through all dermal layers, and there is an increased associated amount of myofibroblasts as seen through immunohistochemistry. Although still an immature scar, these histologic observations suggest that the wounds are developing features similar to hypertrophic scars in humans.[13]

RNA isolation proved difficult after 2 weeks of healing. It is unclear why the total amount of RNA drastically reduced after preparation. It is feasible that cellular content was lacking, or alternatively, an insufficient amount of tissue was provided. Further evaluation is currently under way at our institution regarding the gene expression of these hypertrophic scars.

Limitations to the study are many. The pigs were purchased at a young age predominately for ease of care. The animals grew rapidly with a 100% increase in weight gain over 10 weeks. The rapid change in size and immaturity of age both could have contributed greatly to scar formation and subsequent healing. Scar maturation continues well beyond 10 weeks, and the sampling period was short as evident by the continued increase in erythema at the time of study termination. Providing an absolute even burn to each site was also hindered by a nonflat dorsal surface. We chose the paraspinal area due to minimal surface irregularity. Lastly, it is possible that the scar tissue was too dense; RNA preservation techniques were not able to penetrate the tissue greatly enough to capture all RNA present. This would give false-negative results regarding overall lack of cellularity within these wounds.

CONCLUSIONS

Using a branding iron as a vector of thermal injury inducing excessive scarring, we were successful in creating an immature hypertrophic scar as observed through histology and mechanical evaluations. With the implementation and development of technologies such as the 3D scanner, BTC-2000, and RNA sequencing, more objective and quantifiable data may be obtained when evaluating newer treatment regimens in the management of this difficult clinical problem.

Brian S. Pan, MD
Division of Plastic and Reconstructive Surgery
Shriner's Hospital for Children
Cincinnati Children's Hospital Medical Center
3333 Burnett Avenue
Cincinnati, OH 45229
E-mail: brian.pan@cchmc.org

REFERENCES

1. Zurada JM, Kriegel D, Davis IC. Topical treatments for hypertrophic scars. *J Am Acad Dermatol.* 2006;55:1024–1031.
2. Robert S. English, RS, Shenefelt PD. Keloids and hypertrophic scars. *Dermatol Surg.* 1999;25:632–637.
3. Johnson J, Greenspan B, Gorga D, et al. Compliance with pressure garment use in burn rehabilitation. *J Burn Care Rehabil.* 1994;15:180–188.
4. Macintyre L, Baird M. Pressure garments for use in the treatment of hypertrophic scars—a review of the problems associated with their use. *Burns* 2006;32:10–15.
5. Weinstock-Zlotnick G, Torres-Gray D, Segal R. Effect of pressure garment work gloves on hand function in patients with hand burns: a pilot study. *J Hand Ther.* 2004;17:368–376.
6. Argirova M, Hadjiski O, Wang XQ. Non-operative treatment of hypertrophic scars and keloids after burns in children. *Ann Burns Fire Disasters* 2006;19:1–22.
7. Davis AM, Gerrand C, Griffin A, et al. Evaluation of clinical utility of BTC-2000 for measuring soft tissue fibrosis. *Int J Radiat Oncol Biol Phys.* 2004;60:286–294.
8. Ramos ML, Gragnani A, Ferreira LM. Is there an ideal animal model to study hypertrophic scarring? *J Burn Care Res.* 2008;29:363–368.
9. Meyer W, Schwarz R, Neurand K. The skin of domestic mammals as a model for the human skin, with special reference to the domestic pig. *Curr Probl Dermatol.* 1978;7:39–52.
10. Dorsett-Martin WA. Rat models of skin wound healing: a review. *Wound Repair Regen.* 2004;12:591–599.
11. Lu L, Saulis AS, Liu WR, et al. The temporal effects of anti-TGF-beta1, 2, and 3 monoclonal antibody on wound healing and hypertrophic scar formation. *J Am Coll Surg.* 2005;201:391–397.
12. Liu Y, Chen JY, Shang HT, et al. Light microscopic, electron microscopic, and immunohistochemical comparison of Bama minipig (*Sus scrofa domestica*) and human skin. *Comp Med.* 2010;60:142–148.
13. Momtazi M, Kwan P, Ding J, et al. A nude mouse model of hypertrophic scar shows morphologic and histologic characteristics of human hypertrophic scar. *Wound Repair Regen.* 2013;21:77–87.
14. Cuttle L, Kempf M, Phillips GE, et al. A porcine deep dermal partial thickness burn model with hypertrophic scarring. *Burns* 2006;32:806–820.
15. Sullivan TP, Eaglstein WH, Davis SC, et al. The pig as a model for human wound healing. *Wound Repair Regen.* 2001;9:66–76.
16. Zhu KQ, Engrav LH, Tamura RN, et al. Further similarities between cutaneous scarring in the female, red Duroc pig and human hypertrophic scarring. *Burns* 2004;30:518–530.
17. Liang Z, Engrav LH, Muangman P, et al. Nerve quantification in female red Duroc pig (FRDP) scar compared to human hypertrophic scar. *Burns* 2004;30:57–64.
18. Weinstein GD. Autoradiographic studies on turnover time and protein synthesis in pig epidermis. *J Invest Dermatol.* 1965;44:413–419.
19. Butler KL, Goverman J, Ma H, et al. Stem cells and burns: review and therapeutic implications. *J Burn Care Res.* 2010;31:874–881.
20. Yoshimura K, Shigeura T, Matsumoto D, et al. Characterization of freshly isolated and cultured cells derived from the fatty and fluid portions of liposuction aspirates. *J Cell Physiol.* 2006;208:64–76.
21. Lee SH, Joon HL, Kwang HC, et al. Effects of human adipose-derived stem cells on cutaneous wound healing in nude mice. *Ann Dermatol.* 2011;23:150–155.
22. Bailey JK, Burkes SA, Visscher MO, et al. Multimodal quantitative analysis of early pulsed-dye laser treatment of scars at a pediatric burn hospital. *Dermatol Surg.* 2012;38:1490–1496.
23. Nedelec B, Shankowsky HA, Tredget EE. Rating the resolving hypertrophic scar: comparison of the Vancouver Scar Scale and scar volume. *J Burn Care Rehabil.* 2000;21:205–212.
24. Verhaegen PD, van Zuijlen PP, Pennings NM, et al. Differences in collagen architecture between keloid, hypertrophic scar, normotrophic scar, and normal skin: an objective histopathological analysis. *Wound Repair Regen.* 2009;17:649–656.